ARTICLE

OBC
www.rsc.org/obc

Solution and solid state ^{13}C NMR and X-ray studies of genistein complexes with amines. Potential biological function of the C-7, C-5, and C-4′-OH groups †

Lech Kozerski,*[a,b] Bogdan Kamieński,[b] Robert Kawęcki,[b] Zofia Urbanczyk-Lipkowska,[b] Wojciech Bocian,[a] Elżbieta Bednarek,[a] Jerzy Sitkowski,[a,b] Katarzyna Zakrzewska,[b] Kim T. Nielsen[c] and Poul Erik Hansen*[c]

[a] *National Institute of Public Health, Chelmska 30/34, 00-725 Warsaw, Poland. E-mail: lkoz@icho.edu.pl*

[b] *Institute of Organic Chemistry, Polish Academy of Sciences, Kasprzaka 44, 01-224 Warsaw, Poland*

[c] *Department of Life Sciences and Chemistry, Roskilde University, DK-4000 Roskilde, Denmark*

Received 29th May 2003, Accepted 28th August 2003
First published as an Advance Article on the web 18th September 2003

Parent genistein and its new amine complexes with morpholine and piperazine were studied comparatively in the solid and liquid states by X-ray crystallography and ^{13}C and ^{15}N NMR spectroscopy. Biochanine A and its complexes were used as reference. Secondary deuterium isotope effects on ^{13}C chemical shifts in solution were studied in parent isoflavones and their morpholine and piperazine complexes to aid in evaluation of the electronic distribution in both systems. In addition, to quantify the extent of proton transfer as well as to establish strong hydrogen bonding of the 7-OH group in a morpholine complex, proton transfer from the 7-OH group to the piperazine nitrogen atom was also confirmed by ^{13}C NMR in the solid state and by X-ray studies. The effect of 7-OH deprotonation yields a high frequency shift of 7–8 ppm on the C-7 carbon atom of the piperazine complex whereas it is as large as 12 ppm in the morpholine complex in the solid. The former trend is confirmed from solution state concentration studies which also show that the isoflavones have a strong tendency to form complexes with bases. Depending on the pK_a difference between the isoflavones and the base this leads either to proton transfer and ion-pair formation or, in the case of a larger pK_a difference, to a hydrogen bonded ion pair. The concentration studies show formation of a 1 : 1 genistein–piperazine complex in DMSO. Addition of water leads to formation of solvent separated ions. The C-5 OH group is involved in strong intramolecular hydrogen bonding leading to a pseudo aromatic ring extending the aromatic part of the drug pharmacophore. The analysis also suggests the way that both the C-7 and C-4′ hydroxyl group of genistein may participate in stabilising the ternary inhibitor complexes of tyrosine-specific kinases or DNA topoisomerase II.

Introduction

Parent genistein, 5,7-dihydroxy-3-(4′-hydroxyphenyl)-4*H*-1-benzopyran-4-one, $C_{15}H_{10}O_5$ **1** (Scheme 1) is a natural isoflavone. Recently genistein has raised interest in medical research[1] owing to its diversified interaction with topoisomerase II,[2] as an inhibitor of tyrosine-specific protein kinase[3] or as an immunosuppressant investigated *in vivo*.[4,5] The tyrosine kinase inhibitors also act as antiproliferative agents *in vitro*. Genistein selectively discriminates normal and malignant mononuclear cells in large animals and humans through inhibition of DNA topoisomerase synthesis.[6]

Our previous investigations on the biological activity of various genistein derivatives have shown the amine complexes to exhibit immunosuppressing activity,[4] and induced us to explore the structure of these complexes to find the pharmacophore in the genistein moiety.

Despite the wide interest in the biological activity of genistein and its derivatives,[1] their electronic and geometrical parameters have not been studied in detail. The X-ray structure of genistein[7] and ^1H[8,9] and ^{13}C[10] NMR spectra, and quantum mechanical calculations[11–13] have appeared recently. No

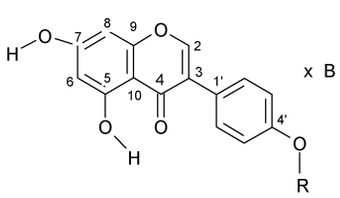

R=H B = none **1**

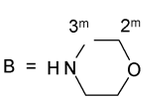

2

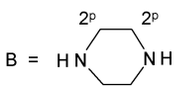

3

R=CH_3 B = none **4**

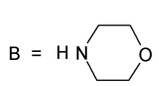

5

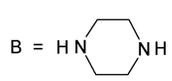

6

Scheme 1

† Electronic supplementary information (ESI) available: table of crystal data and structure refinement for **3**; Fig. 1S: expansion of the high frequency region of ^{13}C solid state spectra of **1**, **2**, **3** and **6**; Fig. 2S: graphs of ^{15}N NMR chemical shifts as a function of water and heavy water addition. See http://www.rsc.org/suppdata/ob/b3/b305991j/

DOI: 10.1039/b305991j

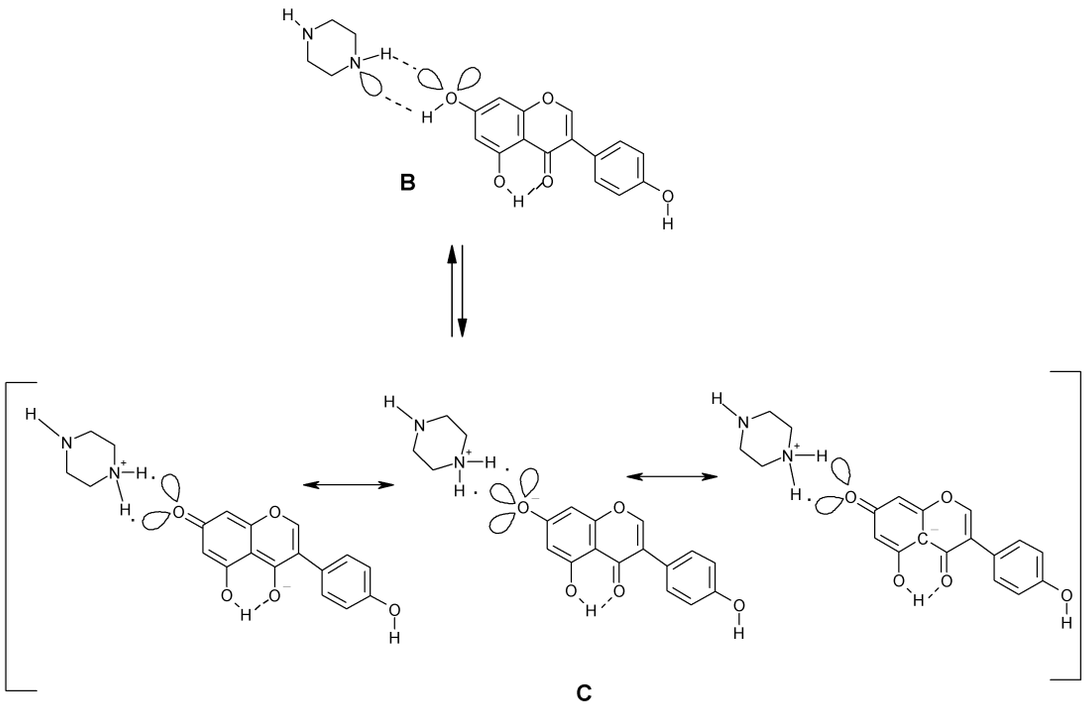

Scheme 2 Proton transfer and complex formation of isoflavone–base complexes

structural information is available with respect to the biological function of the three hydroxyl groups.

The aim of the present study is to compare the structure of genistein **1** and complexes with morpholine **2**, piperazine **3**, (Scheme 1), by X-ray, solid state and solution ^{13}C and ^{15}N NMR including deuterium isotope effects on chemical shifts. These compounds may form very strong hydrogen bonds depending on the pK_a matching of the acid (isoflavone) and the base.[14,15] Comparison of the structure and properties of the parent compound with amine complexes using amines with different basicities may be a way of mapping the domains contributing to its pharmacophore and mimic the specific interactions of the hydroxyl groups with other functional groups in biomolecules leading to hydrogen bonding and proton transfer. The studied compounds are shown in Scheme 1.

A difficulty in using NMR chemical shifts in complexes of the present kind is to differentiate between hydrogen bonding and proton transfer interactions especially if the degree of proton transfer is small. Furthermore, it can also be difficult to distinguish between solvent effects and more specific solute–solute interactions. Isotope effects on chemical shifts have proven useful in establishing the presence of hydrogen bonds.[15,16] In addition, isotope effects on chemical shifts can be used to detect the existence of equilibria.[17]

As these compounds are not very soluble in water it has been customary to use DMSO or acetone as solvent. In order to make the solvent closer to biological conditions a mixture of DMSO/H_2O is attempted in the present paper.

What we achieved in this study was to show in detail how combined NMR techniques applied in solution can yield valuable information on the specific solute–solute interactions. In particular, hydrogen bonding of varying strength can be traced and the position of the proton in the equilibrium can be evaluated. The use of solid state NMR of model systems is also addressed as a source of non-averaged discrete interactions corresponding to those appearing in solution. We believe that this kind of information, applied to the biological systems, is a source of information helpful for construction of models of biomolecule–drug complexes at the atomic level. The ultimate goal is to understand the language of 'living' chemical molecules in biological systems.

Results and discussion

The two components of the complexes **2**, **3**, **5** and **6** may interact in a number of ways by forming complexes and by transfer of protons (see Scheme 2). One suggestion for such an equilibrium is shown in eqn. (1). This shows hydrogen transfer from the isoflavone OH group to the amine in solution.

Depending on the amine pK_a this equilibrium may start from a molecular complex with a hydrogen bond (A) and go to a hydrogen bonded ion pair (C) [eqn. (1)]. This situation can be analysed *e.g.* by means of ^{13}C NMR chemical shifts. However this requires knowledge about the chemical shifts of the involved species, which can in principle be obtained from ^{13}C solid state spectra.

Tracing the hydrogen bond network from the X-ray structure and ^{13}C NMR solid state spectra

In the case of the morpholine complex **2** the X-ray structure is known[13] and shows transfer of the proton. In the present paper the structure of the piperazine complex **3** is determined. The limiting values for the non-transferred case is taken from the solid state spectra of the isoflavones themselves. Crucial for this purpose is the proper assignment of the ^{13}C resonances (see Experimental).

The data in Table 1 show the differential Δ values (difference between chemical shifts of the complex and the isoflavone) for the solid state and for solution. These values for the positions C-7 are characterized by a high frequency shift of 6.8 ppm for **3** and 12 ppm for **2** and reflect the change induced by full proton transfer in the solid and the network of hydrogen bonds which the C-7–O^- oxygen is involved in, as seen in both crystal structures (see below).

$$\underset{A}{\text{Isoflav} + \text{base}} \quad \leftrightarrows \quad \underset{B}{[\text{Isoflav}\cdots \text{base}]} \quad \leftrightarrows \quad \underset{C}{[\text{Isoflav}^{-}\cdots \text{baseH}^{+}]} \qquad (1)$$

Table 1 Comparison of effects on ^{13}C chemical shifts of a transfer from isoflavones genistein (**1**) and biochanin A (**4**) to their complexes with piperazine (Pip) and morpholine (Mor) in the solid state and in DMSO solution[a]

State	Species	δ ^{13}C (ppm)															
		C-1″	C-2″	C2	C3	C4	C5	C6	C7	C8	C9	C10	C1′	C2′*	C3′#	C4′	C5′#	C6′*
Solid[b]	G (**1**)			153.7	124.6	182.2	160.4	97.8	161.2	95.00	157.3	104.2	121.5	133.9	116.9	156.4	116.0	130.2
	G-Pip (**3**)	46.3	45.0	153.9	121.0	180.8	164.5	99.4	168.0	93.80	160.5	105.2	121.0	131.2	118.0	159.2	114.64	129.3
	Δ			0.2	−3.6	−1.4	**+4.1**	+1.6	**+6.8**	−1.2	+3.2	+1.0	−0.5			**+2.8**		
	G-Mor(**2**)	63.7	43.2	154.9	123.2	180.9	162.9	101.7	173.8	94.9	159.7	102.5	121.2	136.0	116.1	158.0		
	Δ			+1.2	−1.4	−1.3	**+2.5**	+3.9	**+12.6**	−0.1	+2.6	−1.7	−0.3			**+1.6**		
	B (**4**)[c]			153.1	119.7	180.8	162.1	100.8	164.4	93.3	157.2	104.1	123.1	131.2	117.3	158.7	110.9	125.9
					120.0	179.6	161.2	98.1		91.6				125.9				
	B[d]-Pip (**6**)	46.3	43.9	153.8	122.4	180.6	163.9	99.2	167.6	93.6	159.5	105.6	123.6	130.5	119.5	161.0	111.0	130.5
	Δ			+0.7					**+3.2**		+2.3	+1.5	+0.5		+2.1	**+2.3**	+0.2	+4.6
Liquid	G (**1**)			153.8	122.2[j]	180.1	161.9	98.9	164.2	93.6	157.5	104.4	121.3[j]	130.0	115.0	157.3		
	Δ S/L			+0.1	−2.2	−1.9	**+1.5**	+1.1	**+3.0**	−1.4	+0.2	+0.2	−0.2	−3.9	−1.9	**+0.9**		
	G-Pip (**3**)	44.9		152.8	121.8*	179.2	161.8	100.4	170.2	94.5	158.0#	102.3	121.6*	130.0	115.0	157.4#		
	Δ			−1.0	−0.4	−0.9	**−0.1**	+1.5	**+6.0**	+0.9	+0.5	−1.9	+0.3	0	0	**0.1**		
	Δ_{tot} [i]	−2.1		−1.8	−0.5	−0.8	**0**	1.8	**6.8**	1.0	0.6	−2.3	0.3	0.1	0.1	**0.3**		
	Δ S/L	−1.4		−1.1	+0.8	−0.8	**+2.7**	+1.0	**+2.2**	+0.7	−2.5	−2.9	+0.6	−1.2	−3.0	**−1.8**		
	G-Mor(**2**)	66.8	45.5	153.5	122.1	179.8	161.9	99.4	166.2	93.9	157.7	103.7	121.3	130.0	115.0	157.3		
	Δ			−0.3	−0.1	−0.3	**0**	+0.5	**+2.0**	+0.3	+0.2	−0.7	0	0	0	**0**		
	ΔS/L	3.1	2.3	−1.4	−1.1	−1.1	**−1.0**	−2.3	**−6.6**	−1.0	−2.0	+1.2	+0.9	−6.0	−1.0	**−0.7**		
	B[e] (**4**)			154.3	121.9	180.1	161.9	99.0	164.3	93.7	157.6	104.4	122.9	130.1	113.6	159.2		
	ΔS/L			+1.2	+2.2	−0.7	**−0.3**	−1.8	**−0.1**	+0.4	+0.4	+0.3	−0.2	−1.1	−3.6	**+0.5**		
	B[f]-Pip (**6**)	45.5	45.5	153.2	121.5	179.2	161.8	100.4	169.6	94.5	158.0	102.6	123.4	130.1	113.6	159.0		
	Δ			−1.1	−0.4	−0.9	**−0.1**	+0.6	**+5.3**	+0.8	+0.4	−1.8	+0.5	0	0	**−0.2**		
	ΔS/L			−0.6	−0.9	−1.4	**−2.1**	+1.2	**+2.0**	+0.9	−1.5	−3.0	0.2	−0.4	−5.9	**−2.0**		
	B[g]-Mor(**5**)	66.7	45.5	153.8	121.9	179.9	**162.0**	99.9	**165.9**	93.2	157.8	103.9	123.0	130.0	113.6	**159.2**		
	Δ			−0.6	0	−0.1	**−0.1**	0.5	**1.5**	−0.5	0.2	−0.5	0.1	−0.1	0	**0**		
	B[h]:Pip(1:6)	46.1		152.2	121.2	178.3	**161.7**	101.6	**173.8**	95.4	158.4	101.0	123.9	130.0	113.6	**158.9**		
	Δ			−2.1	−0.7	−1.8	**−0.2**	2.6	**9.5**	0.9	0.8	−1.6	0.5	−0.1	0	**−0.1**		

[a] Chemical shifts of solid state spectra are calibrated *vs.* glycine as reference; 43.3 ppm, and solution spectra are calibrated *vs.* internal DMSO-d_6, 39.5 ppm, in solutions of 36 mg of a solute in 600 μL of a solvent for all studied species. Signals marked with * or # can be interchanged within the pair; Δ denotes the difference between complex and isoflavone, ΔS/L denotes the difference between respective species in solution and in the solid state. Double prime,″, denotes the carbon atom in bases. [b] See assignment section. [c] Two different molecules in the unit cell. $\delta OCH_3 = 55.7$. [d] $\delta OCH_3 = 57.6$ ppm. [e] $\delta OCH_3 = 55.2$ ppm. [f] $\delta OCH_3 = 55.1$ ppm. [g] $\delta OCH_3 = 55.0$ ppm. [h] $\delta OCH_3 = 55.2$ ppm. [i] Full titration shift as calculated from the concentration curve (Fig. 2a). [j] Assignment reversed compared to ref. 13.

Table 2 Hydrogen-bonds for **3** [Å and deg.]

D–H ··· A	*d*(D–H)	*d*(H ··· A)	*d*(D ··· A)	∠(DHA)
O(5)–H(5) ··· O(4)	1.08(6)	1.58(6)	2.604(5)	157(5)
O(4′)–H(18) ··· O(7)#2	0.88(7)	1.74(7)	2.593(5)	161(7)
N(1″)–H(19) ··· O(5)#3	0.86(7)	2.58(7)	3.110(6)	120(5)
N(4″)–H(20′) ··· O(7)#4	0.95(8)	1.82(8)	2.709(6)	154(6)
N(4″)–H(20) ··· O(6)#5	0.88(9)	2.00(9)	2.814(7)	155(7)
O(2)–H(20A)···O(4)#6	0.96(10)	1.97(11)	2.914(6)	166(9)
O(2)–H(20B) ··· N(1″)#7	0.87(7)	2.08(7)	2.878(7)	151(5)
O(6)–H(21A) ··· O(2)#8	0.87(9)	1.89(9)	2.750(6)	169(8)
O(6)–H(21B) ··· O(7)#9	0.98(9)	1.92(9)	2.893(5)	170(7)
O(3)–H(31) ··· O(4′)#6	1.23(6)	2.28(6)	2.971(12)	112(4)

Symmetry transformations used to generate equivalent atoms: #1 $-x, -y, -z+1$; #2 $x, -y+1/2, z-1/2$; #3 $-x+3/2, y+1/2, z$; #4 $x, y+1, z$; #5 $x-1/2, y, -z+1/2$; #6 $x-1, -y+1/2, z+1/2$; #7 $-x+1, -y+1, -z+1$; #8 $-x+1/2, -y+1, z-1/2$; #9 $x-1/2, y+1, -z+1/2$.

The X-ray structure of **3** has been determined (Fig. 1). The structure shows protonation of the piperazine nitrogen. The C-7–O^- phenolate anion forms three hydrogen bonds, one to NH^+, one to the OH of C-4′ and a third to another NH^+ through hydrogen bonding with a water molecule, thus forming the solvent separated ion pair motif. This motif makes up the main difference in crystal structure packing between **3** and **2** or **1** and can be, in part, responsible for a large difference of C-7 carbon chemical shifts in the solid state spectra of **3** and **2**. The distances and geometries related to hydrogen bonding found in the crystal of **3** are given in Table 2. A comparison of X-ray structures for **1**, **2** and **3** shows that the C-4′ OH is a proton donor in all three crystals. This is reflected in ^{13}C NMR spectra as the change in chemical shifts in going from **1** to **2** and **3** is similar to other carbons, except C-7 (see above), which is involved in proton transfer.

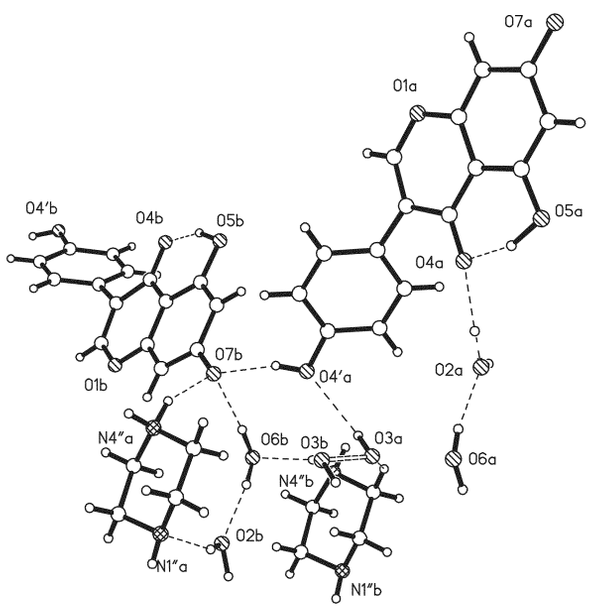

Fig. 1 X-Ray structure of **3**. The O3a and O3b positions show disorder of the water molecule in the crystal.

Tracing the solution equilibria using ^{13}C and ^{15}N chemical shifts

Concentration effects. To gain further insight into the type of interactions between the two components we have studied the concentration dependence of ^{13}C chemical shifts in complexes **2** and **3**. It can be seen that the change in the chemical shift levels off as the concentration increases (Fig. 2). This can best be described by formation of a complex having a proton transfer hydrogen bonded ion-pair type [see eqn. (1), C]. Two features can be ruled out immediately. Genistein is not forming dimers, as no chemical shift changes are found in a concentration

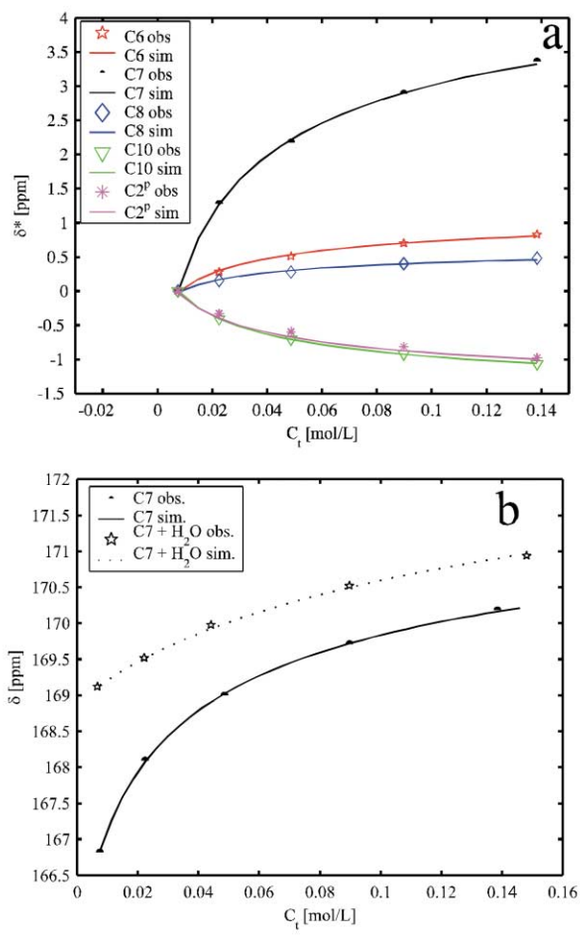

Fig. 2 (a) Concentration dependence of the ^{13}C chemical shift of **3** without added water. The solid line shows fitting according to eqn. (1). Chemical shifts are given on a relative scale. (b) Comparison of chemical shifts of C-7 with and without added water. The solid line shows the fit according to eqn. (1) (without water) and eqn. (2) (with water).

experiment with genistein itself. Secondly, direct proton transfer to form separate isoflavone$^-$ and baseH^+ ions is not taking place as a concentration change in this case is not leading to a shift in the equilibrium. The chemical shifts are dominated by the hydrogen bonded ion-pair [eqn. (1), C]. A least squares fitting of the data based on C in eqn. (1) gives a K_{eq} (A $\leftrightharpoons$ C) of 1 M^{-1} for **2** and one of 50 M^{-1} for **3**. The data can only be fitted assuming a 1 : 1 complex. The calculated chemical shift difference for C-7 is 6.8 ppm for **3**. This coincidence with the solid state data is probably fortuitous. For the piperazine carbon the chemical shift is in the opposite direction, −2.1 ppm (see Table 1 for a full list of all carbon chemical shift differences). For **2** it

Table 3 ^{15}N Chemical shifts in solution and in the solid state

Compounds		Solution state			Solid state
		δ_N	δ_N (ppb)/μl	ΔN(D) (ppm)	
2		−349.13	6.3	0.86	−342.2
3		−347.00	−3.1	0.89 (0.7)[a]	−346.2
Morph	(3.4 M)	−349.13	0.9		
	(1.4 M)	−349.27	1.5		
Pip	(0.33 M)	−347.00	0.5		
	(0.19 M)	−347.00	0.9		
PipHCl	(0.11 M)	−346.50	−1.9		
	(0.09 M)	−346.44	−2.1		

[a] Measured by the MBOB technique with a digital resolution of 0.06 ppm.

is found to be approximately 12 ppm, but in this case the analysis is less precise due to the much smaller chemical shift changes. This is caused by the much smaller binding constant. In both cases the chemical shift of the non-protonated genistein is estimated to be ~165 ppm, a slightly higher value than found for pure genistein in solution. This makes sense as the molecular complex [eqn. (1), B] dominates the chemical shift of the non-charged species. The titration shift derived from this analysis is very close to the numbers found from the solid state spectra (see Table 1).

Effects of water addition. Water addition is done in two ways, either by adding a fixed amount of water (50 μl) to a varying amount of compound (Fig. 2b) or by adding increasing amounts of water to a fixed amount of compound (Fig. 3). In the latter case the effects of adding water to the complex are quite significant. It is also significant that the chemical shifts change in a linear fashion with the amount of water added until it levels off at addition of 200 μl (not shown). The effects observed are akin to those due to complex formation (Δ in Table 1). It is also evident from Fig. 3 that the effects are larger for the piperazine than for the morpholine complex, but in the same direction for both complexes. In Fig. 3 D_2O is added. Addition of H_2O gives the same effect. This was checked for **5**. Interestingly, the effects are rather temperature sensitive. For **5** the effect is almost twice as large for C-7 at 298 K than at 323 K supporting the idea that water influences the position of the equilibrium. Addition of water to the isoflavones themselves (**1** and **4**) has hardly any effect on the chemical shifts.

The ^{15}N chemical shifts in solution show an interesting difference between **2** and **3** upon water addition. The two compounds are different in the sense that piperidine has two nitrogens, only one of which is hydrogen bonded at any time. As only one resonance is observed these two positions must average. This in itself will only lead to a smaller effect. For the former a shift to more positive values is found, whereas for the latter the slope is the opposite (Table 3). Solvent studies of morpholine and piperazine show the same trend pointing to **3** being partially charged (Fig. 2S, ESI). †

In the case when a fixed amount of water was used the data could be analysed by extending eqn. (1) to include a solvent separated ion pair:
Using eqn. (2) leads to a chemical shift for isoflavone$^-$ of the complex [eqn. (2), C] similar to that of the water (solvent) separated one [eqn. (2), D] and to a good fit ‡ of the experimental data (see Fig. 2b). The finding is that the counter ion is not really influencing the ^{13}C chemical shifts.

‡ Standard curve fitting based on a least-squares method was used.

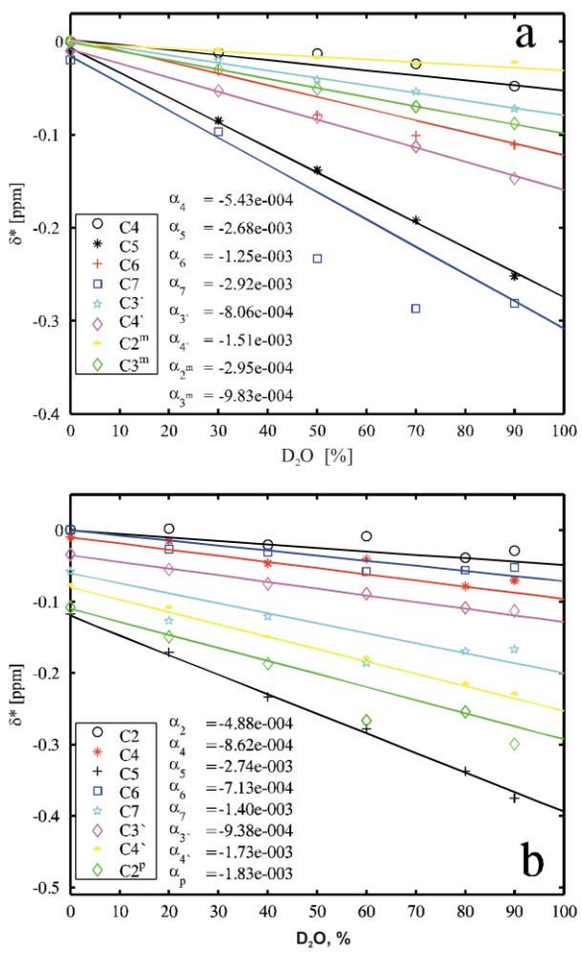

Fig. 3 Plot of ^{13}C chemical shift as a function of percentage of D_2O in the added water: (a) for complex **2**, (b) for complex **3**.

Deuterium isotope effects on chemical shifts. The fine tuning of the problems raised above is accomplished by means of solvent induced isotope effects on ^{13}C chemical shifts. Isotope effect measurement is a well established tool to characterise fast equilibria in solution, *i.e.*, to quantify the position of the given equilibrium and overall electronic distribution.[18] The observed deuterium isotope effects are shown in Table 4.

These data can be used to derive conclusions on the following:

i) Classification of the hydrogen bonds according to their strength

ii) Comparison of the electronic distribution in isoflavones and their complexes

$$\underset{A}{\text{Isoflav} + \text{base}} \leftrightarrows \underset{B}{[\text{Isoflav} \cdot\cdot \text{base}]} \leftrightarrows \underset{C}{[\text{Isoflav}^- \cdot\cdot \text{baseH}^+] + 2\text{H}_2\text{O}} \leftrightarrows \underset{D}{\text{Isoflav}^- \cdot\cdot \text{H}_2\text{O} + \text{baseH}^+ \cdot\cdot \text{H}_2\text{O}} \quad (2)$$

Table 4 Deuterium isotope effects on ^{13}C chemical shifts

Compounds		$^{n}\Delta$ (ppm)																
		C2	C3	C4	C5	C6	C7	C8	C9	C10	C1′	C2′	C3′	C4′	C1″	C2^{m}	C3^{m}	C2^{p}
G[a] (**1**)	298 K	−0.01	0.00	0.00	0.00	0.10	0.20	0.03	0.00	−0.02	−0.03	0.00	0.09	0.16	—	—	—	—
[b]		0.05	−0.05	0.07	0.30	0.03	0.05	−0.06	—	0.02	−0.02	—	—	—	—	—	—	—
G[a] (**1**)	323 K	−0.03	−0.01	−0.02	−0.01	0.09	0.18	0.05	−0.01	−0.05	−0.04	−0.02	0.08	0.14	—	—	—	—
[b]		0.05	−0.05	0.08	0.30	0.03	0.04	−0.06	—	0.02	−0.02	—	—	—	—	—	—	—
G-Mor (**2**)		0.02	−0.07	0.05	0.27	0.13	0.29	−0.01	0.00	−0.03	−0.06	−0.01	0.08	0.15	—	0.03	0.10	—
G-Pip (**3**)	353 K	0.05	−0.04	0.09	0.27	0.07	0.14	−0.03	−0.01	0.05	−0.08	−0.01	0.09	0.17	—	—	—	0.18
	333 K	0.03	−0.05	0.06	0.27	0.07	0.14[f]	−0.03	−0.01	0.01[f]	−0.08	−0.01	0.08	0.16	—	—	—	0.16
	298 K	0.04	−0.09	0.08	0.26	0.06	0.13[f]	−0.03	−0.02	0.05[f]	−0.04	−0.01	0.10	0.17	—	—	—	0.18[f]
B (**4**) [a]		0.00	−0.02	−0.01	0.00	0.07	0.16	0.05	−0.01	−0.01	0.01	−0.01	0.00	0.00	0.00	—	—	—
[b]		0.04	−0.05	0.08	0.30	0.05	0.04	−0.06	—	0.02	−0.02	—	—	—	—	—	—	—
B-Mor (**5**)	333 K	0.02	−0.07	0.05	0.27	—[c]	0.26	—[c]	0.01	−0.04	−0.01	−0.01	0.00	0.00	0.01	—[c]	—[c]	—
	353 K	0.02	−0.07	0.05	0.26	0.13[d]	0.27	−0.01[d]	0.00	−0.03	−0.01	−0.01	0.00	0.00	0.00	0.06[e]	0.10[e]	—
B-Pip (**6**)	323 K	0.08	−0.06	0.08	0.26	—[c]	0.18	—[c]	0.00	0.02	−0.02	0.01	0.01	0.01	0.00	—	—	—[c]
	353 K	0.04	−0.05	0.06	0.29	0.06	0.10	−0.04	0.00	0.02	−0.03	−0.01	0.00	−0.01	0.00	—	—	—[c]
	298 K	0.06	−0.04	0.07	0.24	—[c]	—	—[c]	−0.01	0.07	−0.04	0.00	0.00	0.00	0.00	—	—	—[c]
B : Pip (1 : 6)	323 K	0.10	−0.02	0.11	0.25	−0.03	−0.20	−0.05	−0.03	0.16	−0.06	0.00	0.01	0.01	0.00	—	—	0.15
Mor		—	—	—	—	—	—	—	—	—	—	—	—	—	—	0.04	0.12	—

[a] Isotope effects from C7-OD og C4-OD. [b] Isotope effect from C5-OD. [c] Isotope effects not determined because of asymmetric, broad resonances. [d] Resonances were broad, but symmetrical. [e] Resonances were broad, but not symmetrical (C2^{m} fitted without the last deuterium concentration and C3^{m} without the first). [f] Large uncertainty.

iii) The position of the proton transfer equilibrium in solution of the C-7 and C-4′ sites

The isotope effects fall into two categories; intramolecular hydrogen bonds for the C-5 OH group and intermolecular ones as for C-7 OH and 4′ OH. It is important to notice that except for the isotope effects of OH-5 of the isoflavones (see Experimental) the isotope effects are observed as an average of all effects. The effects at C-5 are of the order of 0.3 ppm in the parent isoflavones and reflect strong intramolecular hydrogen bonding (Table 3). For both genistein and biochanin A large two-bond isotope effects are seen at C-7 whereas C-4′of genistein shows an isotope effect as expected for a simple phenol.[19]

For complexes one has to distinguish between the morpholine and piperazine ones. For **2** none or very little proton transfer is occurring and $^{2}\Delta$C-7(OD)$_{OBS}$ = 0.29 ppm. Part of this is caused by deuteriation at C-5, $^{4}\Delta$C-7(OD-5). The latter can be estimated as 0.05 ppm (taken from genistein), which leaves $^{2}\Delta$C-7(OD-7) as 0.24 ppm. This large value shows that the OH-7 proton is engaged in a rather strong hydrogen bond[20] [molecular complex B, eqn. (1)].

The genistein and biochanin A complexes with piperazin show an isotope effect of ~0.14 ppm on C-7. The $^{2}\Delta$C-7(OD)$_{OBS}$ consists again of the two components, $^{2}\Delta$C-7(OD-7) and $^{4}\Delta$C-7(OD-5) leaving $^{2}\Delta$C-7(OD-7) after subtraction of $^{4}\Delta$C-7(OD-5) (see above) as 0.09 ppm. This smaller value is believed to be due to proton transfer as only part of the hydroxy group is now carrying a proton (deuteron). As the latter has dropped from 0.24 ppm {taken from **2**, which is almost entirely on the molecular complex form [eqn. (1), B] see above} (Table 1) to 0.09 ppm, this corresponds to 38% has a proton at the OH-7 position in **3** at the given concentration.

Deuteriation at the ring in **3** can be taken as evidence for a rather negatively charged O-7, as this will facilitate proton exchange at C-6 and C-8 (Scheme 2) (see Experimental).

Experimental and methods

Genistein and biochanin A were purchased from Sigma and used without purification. Synthesis of complexes **2** and **3** was described earlier.[13] Complexes **5** and **6** were prepared by mixing equimolar amounts of biochanin A and base in ethanol and left for crystallization for a few days. Yellow precipitates were separated and dried under vacuum. The stoichiometry of the complex was checked by ^{1}H NMR. The powder was stable indefinitely, not showing signs of loosing the base. The powder was used for running the spectra in the solid state and in solution.

Concentration studies were accomplished by adding known amounts of a solute to the same volume of solvent, keeping consecutive incremental additions the same for all compounds.

It should also be noticed that upon standing over night deuteriation occurs at both C-6 and C-8 for the genistein–piperazine complex.

^{1}H, ^{13}C and ^{15}N NMR data in solution

The ^{1}H, ^{13}C and ^{15}N NMR measurements were performed in 5 mm tubes using Varian Mercury 300 or INOVA 500 or 600 MHz NMR spectrometers. The ^{1}H and ^{13}C NMR spectra (0.15 mol dm^{-3}) were recorded with DMSO-d$_6$ as a solvent, and TMS as an internal reference. The ^{13}C NMR spectra were run by using a spectral range of 25 kHz, a tip angle of 30°, an acquisition time of 2.56 s, a relaxation delay of 0.5 s and 200–400 transients. Assignments were done using the MBOB sequence.[21]

The ^{15}N NMR spectra (0.15 mol dm^{-3}) were recorded with DMSO-d$_6$ as a solvent and nitromethane as an external reference. The ^{1}H{^{15}N} correlation spectra (g-HMQC[22] — gradient heteronuclear multiple quantum coherence) or selective version of g-HSQC[23] were optimised for a coupling constant of 4 Hz with the following experimental conditions: an acquisition time

of 0.3 s, spectral windows of 4000 (F2) and 500 (F1) Hz, 2048 data points, 512 time increments (zero filled to 2048), a 1.2 s relaxation delay and 2 transients per increment.

Solid state ^{13}C and ^{15}N measurements

The solid state NMR measurements were performed using the standard cross polarization–magic angle spinning (CP–MAS) technique on a Bruker AVANCE 500 DRX spectrometer. A Bruker CP–MAS probe head was used with 4 mm zirconia rotors and a 12 kHz spinning speed. The natural isotopic abundance ^{13}C and ^{15}N spectra were recorded with a $\pi/2$ pulse of 3.2 μs. The ^{13}C spectra were measured at 125.772 MHz under the following conditions: spectral width 31 kHz, contact time 2 ms, acquisition time 25 ms, and relaxation delay 20 s. The short contact cross-polarization (SCP) spectra,[24] presenting the protonated carbon signals only, were measured with a contact time of 40 μs. Typically 250 transients were collected. The spectra were referenced to solid glycine and recalculated to the TMS chemical shift scale using 43.3 ppm for the CH_2 group of glycine.

^{15}N spectra were measured at 50.689 MHz frequency with the following parameters: spectral width 28 kHz, contact time 4 ms, acquisition time 30 ms, and relaxation delay 30 s and 2000 transients. The spectra were referenced to solid glycine and recalculated to the nitromethane chemical shift scale by applying a −347.6 ppm value to the nitrogen signal of glycine.

Assignment techniques in solid state NMR

In the first instance assignment of the ^{13}C NMR solid state spectra is aided by recording short contact time spectra, thereby sorting the proton carrying from the quaternary carbons. The assignment of the quaternary carbons is complicated as the resonances for C-2, C-5, C-7, C-9 and C-4′ fall within a rather narrow chemical shift range both in the isoflavones themselves and in the spectra of the complexes (Table 1). The common practice in the assignment of the solid state spectra is to follow the order of resonances as found in the solution spectra. In the spectra of the complexes we have assigned the resonances of C-2, -3, -4, -5, -9 and -10, which are far from the interaction sites, show deviation from isoflavone spectra of less than 1 ppm. The assignment of C-4′ and C-7 resonances was aided by comparison with spectra of biochanin A, **4**, and its complex **6** and left unassigned C-3′, -5′ and C-2′, -6′, in pairs. The assignment of the genistein–piperazine complex is similar to that arrived at earlier.[25] The relevant chemical shifts are given in Table 1 and are displayed in Fig. 1S.†

Solvent induced isotope effect measurements and assignment

In these experiments we are dealing with isotope effects on the chemical equilibrium, exerted in this particular case by the solvent.[26] Positive effects are to low frequency shifts on deuterium substitution. Deuteriation was achieved by addition of a fixed amount (50 μL) of a mixture of H_2O/D_2O with a varying content of deuterium. Extrapolation from 0 to 100% yields the isotope effects. In the case of ^{15}N deuteriation this was done by an incremental addition of D_2O, examining the ^{15}N NMR spectrum and correcting for the solvent effect (see Fig. 2Sa)† or for **2** by adding a fixed amount of H_2O/D_2O with a varying content of deuterium leading to an isotope effect, $^1\Delta N(D) = 0.66$ ppm.

Deuterium isotope effects on chemical shifts are, in the case of slow exchange on the NMR time scale, observed as two resonances separated by the isotope effect or, in the case of fast exchange, as a change in the chemical shift proportional to the degree of deuteriation.[27] For genistein and biochanin A a combination of the two are found leading to a separation of the isotope effects, due to (OD-5) and (OD-7) as seen in Table 1. The contribution from (OD-4′) can easily be followed as these effects do not extend beyond the phenyl ring. For the complexes the observed isotope effects are the sum of all possible isotope effects at a given carbon. The isotope effects observed for the complexes can be resolved into the individual contributions originating from OD-5, OD-7 and OD-4′. Subtraction of isotope effects observed for the genistein and biochanin A or their complexes give the effects due to (OD-4′) confirming the assignments made above.

X-Ray structure of complex 3

The crystal for X-ray analysis (0.21 × 0.14 × 0.14 mm) was obtained during diffusion crystallization from ethanol in a water chamber. 3026 reflections were measured from the crystal covered by epoxy glue (12.1% decay during measurement) at a Nonius BV MACH3 diffractometer at 150 K using monochromated Cu-Kα radiation. Observed structure factors (F_{obs}^2) were calculated from intensities using the data reduction procedure included in the OpenMoleN system. The structure was solved and refined using SHELXS97[28] and SHELXL97[29] programs, respectively. H-atom positions were found from $\Delta\rho$ maps and refined without constraints. Only one H-atom belonging to the disordered water O3 was found from difference Fourier maps. The C-10 carbon atom that obtained non-positive definition during refinement was given an isotropic thermal parameter. $C_{19}H_{24.5}N_2O_{7.5}$, FW = 400.91, orthorhombic, a = 6.822(1), b = 23.501(5), c = 23.730(5) Å, V = 3804.5(13) Å^3, T = 150 K, space group $Pbca$, Z = 8, μ(Cu-Kα) = 0.915 cm^{-1}, 3026 reflections measured, 1860 independent (R_{int} = 0.0707); final R values: R_1 = 0.0635, wR_2 = 0.1499 for 1705 reflections; $F_{obs} > 2\sigma(I)$.

CCDC reference number 212666.

See http://www.rsc.org/suppdata/ob/b3/b305991j/ for crystallographic data in CIF or other electronic format.

Summary

^{15}N and ^{13}C chemical shifts were measured in the solid state and in solution (in DMSO-d_6, and DMSO-d_6/H_2O mixtures) and the behaviour of the three hydroxy functions at the C-5, C-7 and C-4′ carbons was studied. It was found that the C-5 hydroxy function is involved in strong intramolecular hydrogen bonding of the resonance assisted type and its proton does not participate, as a donor, in an intermolecular hydrogen bond network. Therefore this adds a pseudo-aromatic functionality to the system. In contrast, the C-7 OH group may act a strong hydrogen bond former in cases where no proton transfer is happening, as with weak bases (**2** and **5**), or be partially deprived of the proton in solution as this is transferred to the nitrogen atom (**3** and **6**). The degree of proton transfer depends on the basicity of the base but in both cases the percentage of transfer depends on the concentration. At a concentration of 0.1 M the results of ^{13}C chemical shifts and the isotope effects on chemical shifts show 60–70% transfer in the case of **3**, whereas for **2** the transfer is as low as 10–15%.

In the solid state OH-7 of complex **3** displays the character of a hydroxyl group being both a donor or/and acceptor in a hydrogen bond network. The OH-4′ proton shows no sign of proton transfer in any of the complexes.

Genistein has a well established function as an inhibitor of tyrosine-specific kinases or DNA topoisomerase II. Common for the two inhibition processes is a step of phosphorylation of the tyrosine OH group. In both processes the function and stereochemical placement of the genistein in the interface of the ternary complex, *e.g.*, Gen/DNA/TopoII is not established. Taking into account our findings described above, both the C-7 and C-4′ hydroxyl group may participate in stabilising ternary complexes. Furthermore, as the C-4′ hydroxyl closely resembles the tyrosine function this may divert phosphorylation to genistein and thus be linked covalently to the nucleotide. It is interesting to notice that biochanine A, lacking this OH group, is

not active. The C-7–OH can be viewed as the pharmacophore part of genistein acting as a donor and acceptor in a hydrogen bond network in a ternary complex Gen/DNA/TopoII or being capable of hydrogen transfer to amine functions. The remarkable feature is the complex formation to bases, even weak ones, but of proper pK_a under non-polar conditions. This opens up opportunities for complexation with a number of important interactions with biomolecules, both proteins and nucleic acids at active sites.

Acknowledgements

The authors thank Dr Sc. W. Kozminski (Chemistry Department, Warsaw University) for implementation of the selective version of the g-HSQC pulse program. P. E. H. thanks the Danish Natural Science Research Council for support.

References

1 K. Polkowski and A. P. Mazurek, *Acta Pol. Pharm.-Drug Res.*, 2000, **57**, 135.
2 G. Capranico, M. Palumbo, S. Tinelli, M. Mabilia, A. Pozzan and F. Zunino, *J. Mol. Biol.*, 1994, **235**, 1218.
3 T. Akiyama, J. Ishida, S. Nakagawa, H. Ogawara, S. Watanabe, N. Itoh, M. Shibuya and Y. Fukami, *J. Biol. Chem.*, 1987, **262**, 5592.
4 P. S. Fiedor, M. Maksymowicz, K. Biniecki, L. Kozerski, R. Kawecki, J. Cz. Dobrowolski, J. Pachecka, P. Aranjo, W. Rowinski and A. P. Mazurek, *Congress of European Society for Artificial Organs*, Warsaw, October 17–19, 1996 (Abstract no. 196) p. 3.
5 A. P. Mazurek, K. Biniecki and L. Kozerski, *US Pat.*, 5,637703, June 10, 1997.
6 F. M. Uckun, W. E. Evans, C. J. Forsyth, K. G. Waddick, L. T. Dahlgren, L. M. Chelström, A. Burkhardt, J. Bolen and D. E. Myers, *Science*, 1995, **267**, 886.
7 M. Breton, G. Precigoux, Ch. Courseille and M. Hospital, *Acta Crystallogr., Sect. B*, 1975, **31**, 921.
8 S. Tahara, J. L. Ingham, F. Hanawa and J. Mizutani, *Phytochemistry*, 1991, **30**, 1683.
9 J.-E. Kinjo, J.-I. Furusawa, J. Baba, T. Takeshita, M. Yamasaki and T. Nohara, *Chem. Pharm. Bull.*, 1987, **35**, 4846.
10 A. Pelter, R. S. Ward and R. J. Bass, *J. Chem. Soc., Perkin Trans. 1*, 1978, 666.
11 P. C. Yates, *J. Mol. Struct. (THEOCHEM)*, 1991, **231**, 201.
12 A. P. Mazurek, J. Cz. Dobrowolski, J. Sadlej, E. Bednarek and L. Kozerski, *J. Mol. Struct.*, 2000, **520**, 45.
13 A. P. Mazurek, L. Kozerski, J. Sadlej, R. Kawecki, E. Bednarek, J. Sitkowski, J. Cz. Dobrowolski, J. K. Maurin, K. Biniecki, J. Witkowska, P. Fiedor and J. Pachecka, *J. Chem. Soc., Perkin Trans. 2*, 1998, 1223.
14 W. Kristof and G. Zundel, *Biophys. Struct. Mech.*, 1980, **6**, 209.
15 P. E. Hansen, *Magn. Reson. Chem.*, 1993, **31**, 71.
16 P. E. Hansen, *Magn. Reson. Chem.*, 1993, **31**, 23.
17 S. Bolvig and P. E. Hansen, *Magn. Reson. Chem.*, 1996, **34**, 467.
18 P. E. Hansen, in *Isotope Effects on Chemical Shifts as a Tool in Structural Studies*, H. T. Jensen, ed., Roskilde University Press, Roskilde, 1996.
19 R. A. Newmark and J. R. Hill, *J. Magn. Reson.*, 1976, **21**, 1.
20 P. E. Hansen, M. Christoffersen and S. Bolvig, *Magn. Reson. Chem.*, 1993, **31**, 893.
21 A. Meissner and O. W. Sørensen, *Magn. Reson. Chem.*, 2000, **38**, 981.
22 R. E. Hurd and B. K. John, *J. Magn. Reson.*, 1991, **91**, 648.
23 A. Bax, K. A. Farley and G. S. Walker, *J. Magn. Reson.*, 1996, **A118**, 134.
24 X. Wu, S. T. Burns and K. W. Zilm, *J. Magn. Reson., Ser. A*, 1994, **111**, 29.
25 W. Kolodziejski, A. P. Mazurek and T. Kasprzycka-Gutman, *Chem. Phys. Lett.*, 2000, **328**, 263.
26 L. Kozerski, *Org. Magn. Reson.*, 1982, **20**, 194.
27 P. E. Hansen, *J. Mol. Struct.*, 1994, **321**, 79.
28 G. M. Sheldrick, *Acta Crystallogr., Sect. A*, 1990, **46**, 467–473.
29 G. M. Sheldrick, SHELXL97, Program for Crystal Structure Refinement, University of Göttingen, Germany, 1997.